Shear-Alfven Waves in Gyrokinetic Plasmas

W. W. Lee, J. L. V. Lewandowski, T. S. Hahm, and Z. Lin

Plasma Physics Laboratory, Princeton University, Princeton, NJ 08543

Abstract

It is found that the thermal fluctuation level of the shear-Alfven waves in a gyrokinetic plasma decreases with plasma $\beta(\equiv c_s^2/v_A^2)$, where c_s is the ion acoustic speed and v_A is the Alfven velocity. This unique thermodynamic property based on the fluctuation-dissipation theorem is verified in this paper using a new gyrokinetic particle simulation scheme, which splits the particle distribution function into the equilibrium part as well as the adiabatic and nonadiabatic parts.

PACS numbers: 52.25.Gj, 52.35.Hr, 52.65.Rr, 52.65.Tt

Gyrokinetic particle simulation [1,2] was invented for the purpose of reducing the temporal and spatial disparities in the simulation plasma when one is only interested in the long-wavelength and low-frequency modes in magnetically confined plasmas. Another benefit of the gyrokinetic approach is the reduction of the numerical noise in the simulation [2,3]. On the other hand, the perturbative (δf) particle simulation scheme [4] has made the numerical noise more or less a non-issue, with the argument that one can always make the numerical noise arbitrarily small [5]. In this paper, we will show that the noise issue is still relevant for perturbative gyrokinetic particle simulation when finite-β effects associated with shear-Alfven physics are important. Both analytic and numerical results will be presented. The former is based on the usual fluctuation-dissipation theorem and the latter uses a new simulation scheme which is the finite-β extension of the split-weight perturbative gyrokinetic particle simulation scheme in the electrostatic approximation [6]. Specifically, the new split-weight scheme breaks up the distribution function into an equilibrium part, F_0, as well as an adiabatic part and a non-adiabatic part. The adiabatic part is associated with the product of F_0 and the effective potential of $\psi = \phi + \int \partial A_\| / c\partial t dx_\|$, and the nonadiabatic part is followed dynamically. Here, ϕ is the electrostatic potential, $A_\|$ is the vector potential, and $x_\|$ is the spatial coordinate along the field-line. As we will discuss, without the use of ψ, numerical noise can interfere with the formation of shear-Alfven normal modes.

In the gyrokinetic units of $\rho_s(\equiv \sqrt{\tau}\rho_i)$ and Ω_i^{-1} for length and time, respectively, the governing gyrokinetic Vlasov equation for a finite-β plasma in slab geometry in the limit of $k_\perp^2 \rho_i^2 \ll 1$ can be written as [7]

$$\frac{dF_\alpha}{dt} \equiv \frac{\partial F_\alpha}{\partial t} + v_\| \hat{\mathbf{b}} \cdot \frac{\partial F_\alpha}{\partial \mathbf{x}} - \nabla\phi \times \hat{\mathbf{b}}_0 \cdot \frac{\partial F_\alpha}{\partial \mathbf{x}} + s_\alpha v_{t\alpha}^2 \frac{\partial \psi}{\partial x_\|} \frac{\partial F_\alpha}{\partial v_\|} = 0, \tag{1}$$

where $\tau \equiv T_e/T_i$, α denotes species, $v_{te}^2 = m_i/m_e$, $v_{ti}^2 = 1/\tau$, $s_e = 1$, $s_i = -\tau$,

$$\hat{\mathbf{b}} \equiv \hat{\mathbf{b}}_0 + \frac{\delta \mathbf{B}}{B_0} = \frac{\mathbf{B_0}}{B_0} + \nabla A_\| \times \hat{\mathbf{b}}_0, \tag{2}$$

$$\mathbf{E}^L = -\nabla\phi, \qquad E_\|^T = -\frac{\partial A_\|}{\partial t}, \tag{3}$$

and the superscripts L(ongitudinal) and T(ransverse) denote the decomposition relative to the direction of wave propagation. The effective potential in Eq. (1) is defined as

$$\frac{\partial\psi}{\partial x_\parallel} \equiv -(\mathbf{E}^L + E_\parallel^T \hat{\mathbf{b}}_0)\cdot\hat{\mathbf{b}} = \frac{\partial\phi}{\partial x_\parallel} + \frac{\partial A_\parallel}{\partial t}, \tag{4}$$

and $\partial/\partial x_\parallel \equiv \hat{\mathbf{b}}\cdot\nabla$. The gyrokinetic Poisson's equation for $k_\perp^2\rho_i^2 \ll 1$ can be simplified as

$$\nabla_\perp^2\phi = \int (F_e - F_i)dv_\parallel, \tag{5}$$

where the electrostatic potential ϕ is normalized by T_e/e and $\int F_{0\alpha}dv_\parallel = 1$. Ampere's law then becomes

$$\nabla_\perp^2 A_\parallel = \beta\int v_\parallel(F_e - F_i)dv_\parallel, \tag{6}$$

where the vector potential $A_\parallel$ is normalized by cT_e/ec_s, $\beta \equiv c_s^2/v_A^2$, $v_A \equiv c\lambda_D/\rho_s$ is the Alfven speed, and λ_D is the electron Debye length. [Note that the ion acoustic speed $c_s(\equiv \rho_s\Omega_i)$ is unity in the gyrokinetic unit.] Equations (1)-(6) are the so-called (electromagnetic) Darwin model, in which the transverse induction electric current, $\partial\mathbf{E}^T/\partial t$, is neglected in Ampere's law. The approximation of $J_\parallel^T \approx J_\parallel$ valid for $k_\parallel \ll k_\perp$ is also used here. To expedite the calculation of $\partial\psi/\partial x_\parallel$ of Eq. (4), a generalized Ohm's law in shearless slab geometry, by combining Eqs. (1) - (6), can be written as

$$\left[\nabla_\perp^2 - \beta(\frac{m_i}{m_e}\int F_e dv_\parallel + \int F_i dv_\parallel)\right]\frac{\partial\psi}{\partial x_\parallel} = \beta\frac{\partial}{\partial x_\parallel}\int v_\parallel^2(F_i - F_e)dv_\parallel$$

$$-\beta\nabla\phi\times\hat{\mathbf{b}}_0\cdot\nabla\int v_\parallel(F_i - F_e)dv_\parallel - \frac{\partial}{\partial x_\parallel}\int(F_i - F_e)dv_\parallel. \tag{7}$$

Starting from Eq. (1) and using

$$F_\alpha = F_{0\alpha} + \delta f_\alpha$$

and $\partial F_{0\alpha}/\partial t + v_\parallel\hat{\mathbf{b}}_0\cdot\partial F_{0\alpha}/\partial\mathbf{x} = 0$, we obtain

$$\frac{d\delta f_\alpha}{dt} = -\frac{dF_{0\alpha}}{dt} = s_\alpha v_\parallel\frac{\partial\psi}{\partial x_\parallel}F_{0\alpha}, \tag{8}$$

where d/dt is defined in Eq. (1) and the zeroth-order inhomogeneity is ignored. The generalized Ohm's law, Eq. (7), should then be changed accordingly as

$$[\nabla_\perp^2 - \beta \frac{m_i}{m_e}]\frac{\partial \psi}{\partial x_\parallel} = \beta \frac{\partial}{\partial x_\parallel}\int v_\parallel^2(\delta f_i - \delta f_e) dv_\parallel - \frac{\partial}{\partial x_\parallel}\int (\delta f_i - \delta f_e) dv_\parallel, \tag{9}$$

where the higher order nonlinear terms have been dropped.

The theoretical and numerical properties of the shear-Alfven waves can be studied as follows. The linearized version of Eq. (8),

$$\frac{\partial \delta f_\alpha}{\partial t} + v_\parallel \frac{\partial \delta f_\alpha}{\partial x_\parallel} = s_\alpha v_\parallel \frac{\partial \psi}{\partial x_\parallel} F_{0\alpha}, \tag{10}$$

with the ansatz of $exp(ik_\parallel x_\parallel - i\omega t)$ gives

$$\delta f_\alpha = \left(1 + \frac{\omega}{k_\parallel v_\parallel - \omega}\right) s_\alpha F_{0\alpha}\psi. \tag{11}$$

Substituting it into Eq. (9) and assuming cold ion response of $\omega/k_\parallel \gg v_{ti}$, we obtain the dispersion relation as

$$D \equiv \frac{1}{k^2\lambda_D^2}\left[k_\perp^2 + (1 - \beta\frac{\omega^2}{k_\parallel^2})(1 + X_e)\right] = 0, \tag{12}$$

where D is the dielectric constant for $k^2\lambda_D^2 \ll 1$ and

$$X_\alpha \equiv \frac{\omega}{\sqrt{2}k_\parallel v_{t\alpha}} Z\left(\frac{\omega}{\sqrt{2}k_\parallel v_{t\alpha}}\right).$$

For the cold electron response, $\omega \gg k_\parallel v_{te}$, Eq. (12) gives the normal modes as

$$\omega = \pm \frac{\omega_H}{\sqrt{1 + \omega_{pe}^2/c^2k^2}}, \tag{13}$$

where $c/\omega_{pe}(\equiv \rho_s\sqrt{m_e/m_i\beta})$ is the electron skin depth. In the electrostatic limit of $\omega_{pe}^2/c^2k^2 \rightarrow 0$, it recovers the shear-Alfven modes in the electrostatic limit, i.e., $\omega_H[\equiv (k_\parallel/k_\perp)\sqrt{m_i/m_e}\Omega_i]$ as discussed in Ref. [2]. Equation (13), valid for $\beta \ll m_e/m_i$, shows that the magnitude of the shear-Alfven frequencies becomes lower for higher β's. For the warm electron response of $\omega \ll k_\parallel v_{te}$, the oscillation frequencies from Eq. (12) become

$$\omega = \pm k_\parallel v_A \sqrt{1 + k_\perp^2}, \tag{14}$$

and the corresponding damping rate is

$$\frac{\gamma}{\omega} = -\frac{1}{2}\sqrt{\frac{\pi}{2}}\frac{\omega_l}{k_\parallel v_{te}}\frac{k_\perp^2}{1+k_\perp^2}. \tag{15}$$

where $v_A \equiv \sqrt{1/\beta}$ is the Alfven velocity. These are the kinetic shear-Alfven waves for $\beta \gg m_e/m_i$ and both the magnitude of the frequency and the damping rate continue to decrease for higher β's. For $\beta = 1$, the normal modes are $\omega = \pm k_\parallel c_s \sqrt{1+k_\perp^2}$.

The corresponding fluctuation levels for these modes can be derived as follows. Starting from the fluctuation-dissipation theorem [10] for a system with $\tau = 1$, we can express the thermal fluctuation level as

$$Vk^2|\psi(\mathbf{k})|^2/8\pi = \frac{T_e}{2}\sum_\Omega \frac{1}{|\omega\partial D_R/\partial\omega|_\Omega}, \tag{16}$$

where D_R is the real part of the dielectric constant, Eq. (12), and Ω is the normal mode and V is the volume of the system. For the cold electron response of $\omega \gg k_\parallel v_{te}$, we obtain

$$Vk^2|\psi(\mathbf{k})|^2/8\pi = \frac{T_e}{2}\frac{\lambda_D^2}{\rho_s^2}\frac{1}{1+\omega_{pe}^2/c^2k^2}, \tag{17}$$

and, correspondingly,

$$\left|\frac{e\psi}{T_e}\right| = \frac{1}{\sqrt{N}k\rho_s}\frac{1}{\sqrt{1+\omega_{pe}^2/c^2k^2}}, \tag{18}$$

where N is the number of simulation particles in the waves of interest. Apparently, there is reduction in the noise level as shown in Eq. (18) due to finite-β effects. Equations (17) and (18) are valid for $\beta \ll m_e/m_i$. In the limit of $\beta = 0$ ($\psi \rightarrow \phi$), we recover the level of $|e\phi/T_e| = 1/\sqrt{N}k\rho_s$ as given by Ref. [2,3]. For the warm electron response of $\omega \ll k_\parallel v_{te}$, Eq. (16) gives

$$Vk^2|\psi(\mathbf{k})|^2/8\pi = \frac{T_e}{2}\frac{k^2\lambda_D^2}{1+k^2\rho_s^2}, \tag{19}$$

and, in turn, the noise level becomes

$$\left|\frac{e\psi}{T_e}\right| = \frac{1}{\sqrt{N}}\frac{1}{\sqrt{1+k^2\rho_s^2}}. \tag{20}$$

Thus, Eqs. (19) and (20) indicate that, for $\beta \gg m_e/m_i$, the noise level is much reduced and is nearly constant for $k_\perp^2\rho_s^2 \ll 1$. For $\beta = 0$ with warm electrons and cold ions, Eq. (12) gives the normal mode of $\omega = \pm k_\parallel c_s/\sqrt{1+k^2\rho_s^2}$, which is the gyrokinetic version of the ion acoustic waves and its thermal energy and noise level are the same as those given in Eqs. (19) and (20) with ψ replaced by ϕ. For $k^2\rho_s^2 \ll 1$, we recover the noise level for the usual ion acoustic waves.

The total fluctuation level in a finite-β gyrokinetic plasma can be obtained by integrating over the the whole ω spectra [3], i.e.,

$$Vk^2|\psi(\mathbf{k})|^2/8\pi = \frac{T}{2}\left(\frac{1}{D(\omega=\infty)} - \frac{1}{D(\omega=0)}\right) = \frac{T_e}{2}\frac{\lambda_D^2}{\rho_s^2}. \tag{21}$$

The corresponding fluctuation potential becomes

$$\left|\frac{e\psi}{T_e}\right| = \frac{1}{\sqrt{N}k\rho_s}. \tag{22}$$

These levels are the same as those obtained earlier for finite-β plasmas [8,11] and are also the same as the electrostatic cases [2,3]. Thus, there is no reduction in the total noise level due to finite β effects. However, as shown in Eqs. (17)-(20), noise reduction indeed exists, but only for the shear-Alfven normal modes. The difference comes from the fact that, in a gyrokinetic plasma, there is no damping mechanism to reduce the noise produced by the fast moving electrons.

The interest in utilizing the desirable numerical properties of shear-Alfven waves for simulation purposes was first mentioned in Ref. [12]. However, a simple application of the perturbative δf scheme [4] to solve Eqs. (8) and (9) was limited to low β plasmas, i.e., $\beta \le m_e/m_i$. The subsequent work [9] using the canonical momentum as a phase space variable [7] encountered similar restrictions. In both cases, numerical noise was cited as a possible suspect - in agreement with our analyses presented here. Namely, the interference of the nonadiabatic responses of the fast electrons with the collective oscillations of shear-Alfven waves is the culprit.

To prove this point numerically, we have devised a new simulation scheme, which is the extension of the split-weight δf scheme [6] to finite-β plasmas. Briefly, the scheme divides the perturbed electron distribution into the adiabatic and non-adiabatic parts, i.e.,

$$\delta f_e = \psi F_{0e} + \delta h_e.$$

From $d\psi/dt = \partial\psi/\partial t + v_\parallel \hat{\mathbf{b}} \cdot \partial\psi/\partial\mathbf{x} - \nabla\phi \times \hat{\mathbf{b}}_0 \cdot \partial\psi/\partial\mathbf{x}$ and Eq. (1), and dropping the nonlinear terms, we obtain

$$\frac{d\delta h_e}{dt} = -\frac{\partial\psi}{\partial t} F_{0e}. \tag{23}$$

Defining

$$w^{NA} \equiv \delta h_e / F_e,$$

the weight equation can then be written as

$$\frac{dw^{NA}}{dt} = \frac{1}{F_e}\frac{d\delta h_e}{dt} = -\frac{1 - w^{NA}}{1+\psi}\frac{\partial\psi}{\partial t}. \tag{24}$$

The corresponding equations of motion are

$$\frac{d\mathbf{x}}{dt} = v_\parallel \hat{\mathbf{b}}_0 - \nabla(\phi - v_\parallel A_\parallel) \times \hat{\mathbf{b}}_0, \tag{25}$$

$$\frac{dv_\parallel}{dt} = s_\alpha v_{t\alpha}^2 \frac{\partial\psi}{\partial x_\parallel}, \tag{26}$$

and the generalized Ohm's law is simplified as

$$(\nabla_\perp^2 - 1)\frac{\partial\psi}{\partial x_\parallel} = \beta\frac{\partial}{\partial x_\parallel}\int v_\parallel^2(\delta f_i - \delta h_e)dv_\parallel - \frac{\partial}{\partial x_\parallel}\int(\delta f_i - \delta h_e)dv_\parallel. \tag{27}$$

where the perturbed ion distribution, δf_i, can be calculated by the standard δf scheme [4] and the nonadiabatic electron contribution is given by

$$\delta h_e = \sum_{j=1}^{N} w_j^{NA}\delta(\mathbf{x} - \mathbf{x}_j)\delta(v_\parallel - v_{\parallel j}).$$

Taking $\partial/\partial t$ of Eqs. (9) and (27) and using Eqs. (8) and (23), we arrive at

$$[\nabla_\perp^2 - \beta\frac{m_i}{m_e}]\frac{\partial\psi}{\partial t} = -\beta\frac{\partial}{\partial x_\parallel}\int v_\parallel^3(\delta f_i - \delta h_e)dv_\parallel + \frac{\partial}{\partial x_\parallel}\int v_\parallel(\delta f_i - \delta h_e)dv_\parallel. \tag{28}$$

Equations (24)-(28) form the basic set for finite-β split-weight particle simulation.

The simulation has been carried out with a one dimensional simulation code, GK1D. In the code, both x and z are ignorable coordinates, $y = \theta x_\parallel$, and $\theta \ll 1$ is the angle between the external B field and the z axis. This is a linear simulation in which Eqs. (24) - (26) are simplified to $dx_\parallel/dt = v_\parallel$, $dv_\parallel/dt = 0$, and $dw^{NA}/dt = -\partial\psi/\partial t$, respectively. The simulation uses a 64 grid system with 6765 particles and includes only the modes with $k\rho_s \approx \pm 0.4$. The other parameters are: $m_i/m_e = 1837$, $\tau = 1$, $\theta = 0.01$, and a (particle size) $= 0$. In all the simulations reported here, we set the initial amplitude to $e\psi/T_e = 100\%$. In Fig. 1, the fluctuation (noise) levels and frequencies for the $\beta = 0$ case are shown, where $\Omega_i \Delta t = 0.2$ is the time step used in the simulation. The noise level of $e\psi/T_e \simeq 3\%$ at $\Omega_i t = 60$ agrees well with that given by Eq. (18). However, the noise fluctuates wildly in the ensuing simulation and reaches as high as 20% at times. This unphysically high amplitude of oscillations increases with larger time steps. Furthermore, the simulation frequencies shown in Fig. 1 are slightly higher than the theoretical values given by Eq. (13), probably due to the enhanced noise as well. The results for the case of $\beta = 0.1\%$ are shown in Fig. 2, where $\Omega_i \Delta t = 2$ is used. Both the linear frequencies and the damping rate of $(\omega + i\gamma)/\Omega_i = \pm 0.13 - i0.011$ are in good agreement with the theoretical predictions of Eqs. (14) and (15). In the steady state, the noise level improves to $e\psi/T_e \simeq 1.2\%$ and also agrees with the amplitude predicted by Eq. (20) and there is no numerical enhancement. For $\beta = 10\%$ and $\Omega_i \Delta t = 2$, the frequencies and the damping rate of $(\omega + i\gamma)/\Omega_i = \pm 0.014 - i0.00012$, as given by Fig. 3, are in excellent agreement with those from Eqs. (14) and (15). For the last two cases, the time step is restricted by the parallel transit time requirement of $k_\parallel v_{te} \Delta t < 1$ [2].

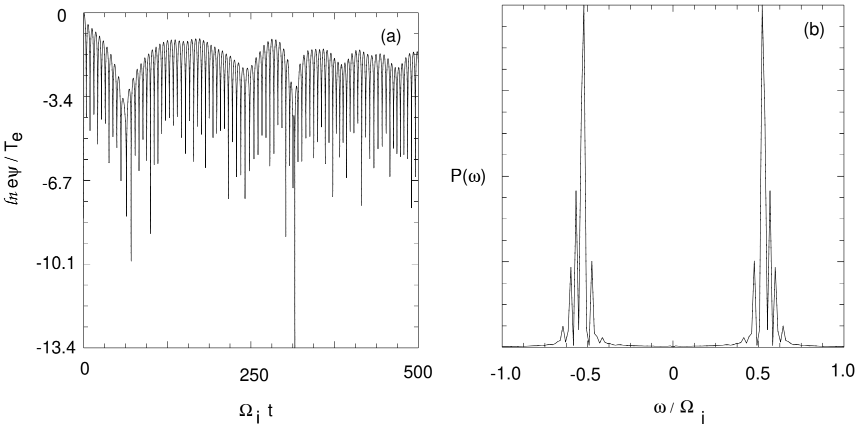

Figure 1. (a) Damping rate and noise level, and (b) frequencies for the shear-Alfven waves for $\beta = 0.0\%$

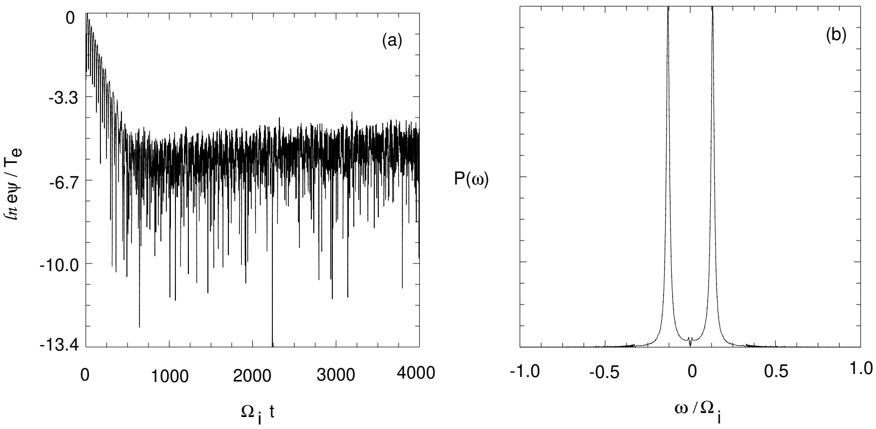

Figure 2. (a) Damping rate and noise level, and (b) frequencies for the shear-Alfven waves for $\beta = 0.1\%$

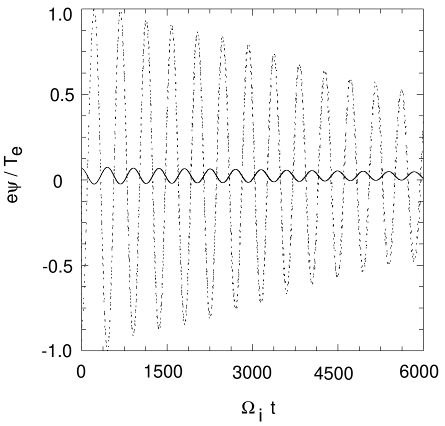

Figure 3. Shear-Alfven oscillations for $\beta = 10.0\%$

In conclusion, we believe that we have finally resolved a decade old puzzle concerning the favorable numerical trend for a finite-β gyrokinetic plasma [12], which is found here to be intimately related to the unique thermodynamic feature of the shear-Alfven waves. Without such an understanding, one would conclude from Eq. (22) [8,11] that finite-β gyrokinetic particle simulation of long wavelength modes with $k\rho_s \rightarrow 0$ is nearly impossible. Most of all, we have developed a new simulation scheme that can be generalized to multi-dimensional simulations of finite-β plasmas.

The research was supported by the Plasma Science Accelerated Computing Initiative of the U. S. DoE.

REFERENCES

[1] W. W. Lee, Phys. Fluids **26**, 556 (1983).

[2] W. W. Lee, J. Comput. Phys. **72**, 243 (1987).

[3] J. A. Krommes, W. W. Lee and C. Oberman, Phys. Fluids **29**, 2421 (1986).

[4] S. E. Parker and W. W. Lee, Phys. Fluids B **5**, 77 (1993).

[5] G. Hu and J. A. Krommes, Phys. plasmas **1**, 863 (1994).

[6] I. Manuilskiy and W. W. Lee, Phys. Plasmas **7**, 1381 (2000).

[7] T. S. Hahm, W. W. Lee and A. Brizard, Phys. Fluids **31**, 1940 (1987).

[8] J. V. W. Reynders, Ph.D. thesis, Princeton University (1992).

[9] J. C. Cummings, Ph.D. thesis, Princeton University (1995).

[10] Yu. L. Klimontovich, *The statistical Theory of Non-Equilibrium Processes in a Plasma*, (MIT Press, 1967).

[11] J. A. Krommes, Phys. Rev. Lett. **70**, 3067 (1993); *ibid.* Phys. Fluids B **5**, 2405 (1993); *ibid.* Phys. Fluids B **5**, 1066 (1993).

[12] W. W. Lee, T. S. Hahm and J. V. W. Reynders, Bull. Am. Phys. Soc. **34**, 2044 (1989).